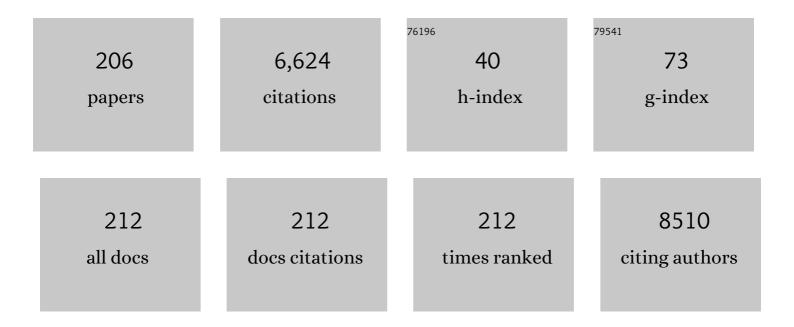
List of Publications by Year in descending order

Source: https://exaly.com/author-pdf/5424598/publications.pdf Version: 2024-02-01



#	Article	IF	CITATIONS
1	Sleep and perivascular spaces in the middleâ€aged and elderly population. Journal of Sleep Research, 2022, 31, e13485.	1.7	9
2	An end-to-end approach to segmentation in medical images with CNN and posterior-CRF. Medical Image Analysis, 2022, 76, 102311.	7.0	16
3	Diaphragmatic dysfunction in neuromuscular disease, an MRI study. Neuromuscular Disorders, 2022, 32, 15-24.	0.3	5
4	Bronchial wall parameters on CT in healthy never-smoking, smoking, COPD, and asthma populations: a systematic review and meta-analysis. European Radiology, 2022, 32, 5308-5318.	2.3	5
5	Deep learning methods for automatic evaluation of delayed enhancement-MRI. The results of the EMIDEC challenge. Medical Image Analysis, 2022, 79, 102428.	7.0	16
6	Chest MRI to diagnose early diaphragmatic weakness in Pompe disease. Orphanet Journal of Rare Diseases, 2021, 16, 21.	1.2	7
7	Developing and validating COVID-19 adverse outcome risk prediction models from a bi-national European cohort of 5594 patients. Scientific Reports, 2021, 11, 3246.	1.6	62
8	Crowdsourcing airway annotations in chest computed tomography images. PLoS ONE, 2021, 16, e0249580.	1.1	1
9	Automatic airway segmentation from computed tomography using robust and efficient 3-D convolutional neural networks. Scientific Reports, 2021, 11, 16001.	1.6	14
10	Automated Segmentation and Volume Measurement of Intracranial Internal Carotid Artery Calcification at Noncontrast CT. Radiology: Artificial Intelligence, 2021, 3, e200226.	3.0	9
11	Intracranial arteriosclerosis is related to cerebral small vessel disease: a prospective cohort study. Neurobiology of Aging, 2021, 105, 16-24.	1.5	5
12	Adversarial attack vulnerability of medical image analysis systems: Unexplored factors. Medical Image Analysis, 2021, 73, 102141.	7.0	35
13	Assessment of fully automatic segmentation of pulmonary artery and aorta on noncontrast CT with optimal surface graph cuts. Medical Physics, 2021, 48, 7837.	1.6	5
14	Creating a training set for artificial intelligence from initial segmentations of airways. European Radiology Experimental, 2021, 5, 54.	1.7	3
15	Learning to Quantify Emphysema Extent: What Labels Do We Need?. IEEE Journal of Biomedical and Health Informatics, 2020, 24, 1149-1159.	3.9	2
16	Growth of the thoracic aorta in the smoking population: The Danish Lung Cancer Screening Trial. International Journal of Cardiology, 2020, 299, 276-281.	0.8	7
17	Classification of Volumetric Images Using Multi-Instance Learning and Extreme Value Theorem. IEEE Transactions on Medical Imaging, 2020, 39, 854-865.	5.4	13
18	Three-dimensional ultrasound evaluation of the effects of pomegranate therapy on carotid plaque texture using locality preserving projection. Computer Methods and Programs in Biomedicine, 2020, 184, 105276.	2.6	12

#	Article	IF	CITATIONS
19	Longitudinal assessment of carotid plaque texture in three-dimensional ultrasound images based on semi-supervised graph-based dimensionality reduction and feature selection. Computers in Biology and Medicine, 2020, 116, 103586.	3.9	11
20	Weakly supervised object detection with 2D and 3D regression neural networks. Medical Image Analysis, 2020, 65, 101767.	7.0	27
21	Spectral Data Augmentation Techniques to Quantify Lung Pathology from CT-Images. , 2020, , .		3
22	Graph refinement based airway extraction using mean-field networks and graph neural networks. Medical Image Analysis, 2020, 64, 101751.	7.0	15
23	Airway tapering: an objective image biomarker for bronchiectasis. European Radiology, 2020, 30, 2703-2711.	2.3	19
24	Multi-atlas image registration of clinical data with automated quality assessment using ventricle segmentation. Medical Image Analysis, 2020, 63, 101698.	7.0	25
25	Chronic Obstructive Pulmonary Disease Quantification Using CT Texture Analysis and Densitometry: Results From the Danish Lung Cancer Screening Trial. American Journal of Roentgenology, 2020, 214, 1269-1279.	1.0	22
26	Region-of-Interest Guided Supervoxel Inpainting for Self-supervision. Lecture Notes in Computer Science, 2020, , 500-509.	1.0	3
27	Transfer Learning for Image Segmentation by Combining Image Weighting and Kernel Learning. IEEE Transactions on Medical Imaging, 2019, 38, 213-224.	5.4	66
28	Extracting tree structures in CT data by tracking multiple statistically ranked hypotheses. Medical Physics, 2019, 46, 4431-4440.	1.6	1
29	Gray Matter Age Prediction as a Biomarker for Risk of Dementia. Proceedings of the National Academy of Sciences of the United States of America, 2019, 116, 21213-21218.	3.3	147
30	The value of hippocampal volume, shape, and texture for 11-year prediction of dementia: a population-based study. Neurobiology of Aging, 2019, 81, 58-66.	1.5	8
31	Reference values and variation of acetabular angles measured by computed tomography in 170 asymptomatic hips. Acta Radiologica, 2019, 60, 895-901.	0.5	4
32	Not-so-supervised: A survey of semi-supervised, multi-instance, and transfer learning in medical image analysis. Medical Image Analysis, 2019, 54, 280-296.	7.0	545
33	Automated 3D segmentation and diameter measurement of the thoracic aorta on non-contrast enhanced CT. European Radiology, 2019, 29, 4613-4623.	2.3	45
34	Learning Cross-Modality Representations From Multi-Modal Images. IEEE Transactions on Medical Imaging, 2019, 38, 638-648.	5.4	40
35	Technical challenges of quantitative chest MRI data analysis in a large cohort pediatric study. European Radiology, 2019, 29, 2770-2782.	2.3	6
36	3D regression neural network for the quantification of enlarged perivascular spaces in brain MRI. Medical Image Analysis, 2019, 51, 89-100.	7.0	42

#	Article	IF	CITATIONS
37	Increasing Accuracy of Optimal Surfaces Using Min-Marginal Energies. IEEE Transactions on Medical Imaging, 2019, 38, 1559-1568.	5.4	2
38	Enlarged perivascular spaces in brain MRI: Automated quantification in four regions. Neurolmage, 2019, 185, 534-544.	2.1	77
39	A Cross-Center Smoothness Prior for Variational Bayesian Brain Tissue Segmentation. Lecture Notes in Computer Science, 2019, , 360-371.	1.0	6
40	Semi-supervised Medical Image Segmentation via Learning Consistency Under Transformations. Lecture Notes in Computer Science, 2019, , 810-818.	1.0	91
41	Automated Lesion Detection byÂRegressing Intensity-Based Distance withÂa Neural Network. Lecture Notes in Computer Science, 2019, , 234-242.	1.0	13
42	Hydranet: Data Augmentation for Regression Neural Networks. Lecture Notes in Computer Science, 2019, , 438-446.	1.0	5
43	A Joint 3D UNet-Graph Neural Network-Based Method for Airway Segmentation from Chest CTs. Lecture Notes in Computer Science, 2019, , 583-591.	1.0	27
44	Automated Quantification of Enlarged Perivascular Spaces in Clinical Brain MRI Across Sites. Lecture Notes in Computer Science, 2019, , 103-111.	1.0	1
45	Maximization of regional probabilities using Optimal Surface Graphs: Application to carotid artery segmentation in MRI. Medical Physics, 2018, 45, 1159-1169.	1.6	11
46	lmaging of respiratory muscles in neuromuscular disease: A review. Neuromuscular Disorders, 2018, 28, 246-256.	0.3	21
47	Detecting emphysema with multiple instance learning. , 2018, , .		8
48	Automatic emphysema detection using weakly labeled HRCT lung images. PLoS ONE, 2018, 13, e0205397.	1.1	17
49	Cooperative carotid artery centerline extraction in MRI. PLoS ONE, 2018, 13, e0197180.	1.1	2
50	Transfer Learning for Multicenter Classification of Chronic Obstructive Pulmonary Disease. IEEE Journal of Biomedical and Health Informatics, 2018, 22, 1486-1496.	3.9	57
51	Transfer learning by feature-space transformation: A method for Hippocampus segmentation across scanners. Neurolmage: Clinical, 2018, 20, 466-475.	1.4	7
52	Reliability of computer-assisted periacetabular osteotomy using a minimally invasive approach. International Journal of Computer Assisted Radiology and Surgery, 2018, 13, 2021-2028.	1.7	8
53	Deep Learning from Label Proportions for Emphysema Quantification. Lecture Notes in Computer Science, 2018, , 768-776.	1.0	10
54	Quantification of lung abnormalities in cystic fibrosis using deep networks. , 2018, , .		7

4

#	Article	IF	CITATIONS
55	Aorta and pulmonary artery segmentation using optimal surface graph cuts in non-contrast CT. , 2018, , .		6
56	Diagnosis of bronchiectasis and airway wall thickening in children with cystic fibrosis: Objective airway-artery quantification. European Radiology, 2017, 27, 4680-4689.	2.3	55
57	Comparison of ct and MRI on the detection and quantification of carotid artery calcification: The rotterdam study. Atherosclerosis, 2017, 263, e17.	0.4	Ο
58	Representation Learning for Cross-Modality Classification. Lecture Notes in Computer Science, 2017, , 126-136.	1.0	4
59	Automated Registration of Freehand B-Mode Ultrasound and Magnetic Resonance Imaging of the Carotid Arteries Based on Geometric Features. Ultrasound in Medicine and Biology, 2017, 43, 273-285.	0.7	6
60	Objective airway artery dimensions compared to CT scoring methods assessing structural cystic fibrosis lung disease. Journal of Cystic Fibrosis, 2017, 16, 116-123.	0.3	25
61	Extraction of Airways with Probabilistic State-Space Models and Bayesian Smoothing. Lecture Notes in Computer Science, 2017, , 53-63.	1.0	3
62	Fully Automated Lung Volume Assessment from MRI in a Population-based Child Cohort Study. , 2017, , .		2
63	Segmentation of Intracranial Arterial Calcification with Deeply Supervised Residual Dropout Networks. Lecture Notes in Computer Science, 2017, , 356-364.	1.0	6
64	Crowdsourced Emphysema Assessment. Lecture Notes in Computer Science, 2017, , 126-135.	1.0	3
65	Quantification of Diaphragm Mechanics in Pompe Disease Using Dynamic 3D MRI. PLoS ONE, 2016, 11, e0158912.	1.1	30
66	Automatic airway–artery analysis on lung CT to quantify airway wall thickening and bronchiectasis. Medical Physics, 2016, 43, 5736-5744.	1.6	38
67	The development of bronchiectasis on chest computed tomography in children with cystic fibrosis: can pre-stages be identified?. European Radiology, 2016, 26, 4563-4569.	2.3	18
68	High shear stress relates to intraplaque haemorrhage in asymptomatic carotid plaques. Atherosclerosis, 2016, 251, 348-354.	0.4	79
69	Multicentre chest computed tomography standardisation in children and adolescents with cystic fibrosis: the way forward. European Respiratory Journal, 2016, 47, 1706-1717.	3.1	44
70	Machine learning approaches in medical image analysis: From detection to diagnosis. Medical Image Analysis, 2016, 33, 94-97.	7.0	231
71	Relation between wall shear stress and carotid artery wall thickening MRI versus CFD. Journal of Biomechanics, 2016, 49, 735-741.	0.9	41
72	Combining Generative and Discriminative Representation Learning for Lung CT Analysis With Convolutional Restricted Boltzmann Machines. IEEE Transactions on Medical Imaging, 2016, 35, 1262-1272.	5.4	116

#	Article	lF	CITATIONS
73	Carotid Artery Wall Segmentation in Multispectral MRI by Coupled Optimal Surface Graph Cuts. IEEE Transactions on Medical Imaging, 2016, 35, 901-911.	5.4	29
74	Visual assessment of early emphysema and interstitial abnormalities on CT is useful in lung cancer risk analysis. European Radiology, 2016, 26, 487-494.	2.3	42
75	Comparison of CT and CMR for detection and quantification of carotid artery calcification: the Rotterdam Study. Journal of Cardiovascular Magnetic Resonance, 2016, 19, 28.	1.6	12
76	Early Experiences with Crowdsourcing Airway Annotations in Chest CT. Lecture Notes in Computer Science, 2016, , 209-218.	1.0	15
77	Reply: Excess Risk of Cancer from Computed Tomography Scan Is Small but Not So Low as to Be Incalculable. American Journal of Respiratory and Critical Care Medicine, 2015, 192, 1397-1399.	2.5	6
78	MRBrainS Challenge: Online Evaluation Framework for Brain Image Segmentation in 3T MRI Scans. Computational Intelligence and Neuroscience, 2015, 2015, 1-16.	1.1	179
79	Geodesic Atlas-Based Labeling of Anatomical Trees: Application and Evaluation on Airways Extracted From CT. IEEE Transactions on Medical Imaging, 2015, 34, 1212-1226.	5.4	17
80	Multi-Center MRI Carotid Plaque Component Segmentation Using Feature Normalization and Transfer Learning. IEEE Transactions on Medical Imaging, 2015, 34, 1294-1305.	5.4	28
81	Transfer Learning Improves Supervised Image Segmentation Across Imaging Protocols. IEEE Transactions on Medical Imaging, 2015, 34, 1018-1030.	5.4	191
82	Reversibility of trapped air on chest computed tomography in cystic fibrosis patients. European Journal of Radiology, 2015, 84, 1184-1190.	1.2	22
83	Weighting training images by maximizing distribution similarity for supervised segmentation across scanners. Medical Image Analysis, 2015, 24, 245-254.	7.0	23
84	PRAGMA-CF. A Quantitative Structural Lung Disease Computed Tomography Outcome in Young Children with Cystic Fibrosis. American Journal of Respiratory and Critical Care Medicine, 2015, 191, 1158-1165.	2.5	192
85	Lung MRI and impairment of diaphragmatic function in Pompe disease. BMC Pulmonary Medicine, 2015, 15, 54.	0.8	42
86	Why Does Synthesized Data Improve Multi-sequence Classification?. Lecture Notes in Computer Science, 2015, , 531-538.	1.0	34
87	Letter by Bos et al Regarding Article, "Intracranial Carotid Calcification on Cranial Computed Tomography: Visual Scoring Methods, Semiautomated Scores, and Volume Measurements in Patients With Stroke― Stroke, 2015, 46, e254.	1.0	3
88	Quantification and Visualization of Variation in Anatomical Trees. Association for Women in Mathematics Series, 2015, , 57-79.	0.1	5
89	Feature-Space Transformation Improves Supervised Segmentation Across Scanners. Lecture Notes in Computer Science, 2015, , 85-93.	1.0	1
90	Label Stability in Multiple Instance Learning. Lecture Notes in Computer Science, 2015, , 539-546.	1.0	8

#	Article	IF	CITATIONS
91	Classification of COPD with Multiple Instance Learning. , 2014, , .		25
92	Spirometer-controlled cine magnetic resonance imaging used to diagnose tracheobronchomalacia in paediatric patients. European Respiratory Journal, 2014, 43, 115-124.	3.1	40
93	Atherosclerotic Plaque Component Segmentation in Combined Carotid MRI and CTA Data Incorporating Class Label Uncertainty. PLoS ONE, 2014, 9, e94840.	1.1	25
94	Three-Dimensional Carotid Ultrasound Plaque Texture Predicts Vascular Events. Stroke, 2014, 45, 2695-2701.	1.0	83
95	Learning Features for Tissue Classification with the Classification Restricted Boltzmann Machine. Lecture Notes in Computer Science, 2014, , 47-58.	1.0	16
96	Hippocampal shape is predictive for the development of dementia in a normal, elderly population. Human Brain Mapping, 2014, 35, 2359-2371.	1.9	52
97	Evaluation of automated statistical shape model based knee kinematics from biplane fluoroscopy. Journal of Biomechanics, 2014, 47, 122-129.	0.9	34
98	Effect of inspiration on airway dimensions measured in maximal inspiration CT images of subjects without airflow limitation. European Radiology, 2014, 24, 2319-2325.	2.3	16
99	Optimal surface segmentation using flow lines to quantify airway abnormalities in chronic obstructive pulmonary disease. Medical Image Analysis, 2014, 18, 531-541.	7.0	28
100	Nonrigid Registration of Volumetric Images Using Ranked Order Statistics. IEEE Transactions on Medical Imaging, 2014, 33, 422-432.	5.4	5
101	Quantification of Smoothing Requirement for 3D Optic Flow Calculation of Volumetric Images. IEEE Transactions on Image Processing, 2013, 22, 2128-2137.	6.0	5
102	Toward a Theory of Statistical Tree-Shape Analysis. IEEE Transactions on Pattern Analysis and Machine Intelligence, 2013, 35, 2008-2021.	9.7	39
103	Local appearance features for robust MRI brain structure segmentation across scanning protocols. , 2013, , .		2
104	Statistical coronary motion models for 2D+t/3D registration of X-ray coronary angiography and CTA. Medical Image Analysis, 2013, 17, 698-709.	7.0	42
105	Automated measurement of diagnostic angles for hip dysplasia. , 2013, , .		6
106	Chest computed tomography: a validated surrogate endpoint of cystic fibrosis lung disease?. European Respiratory Journal, 2013, 42, 844-857.	3.1	36
107	Automated segmentation of atherosclerotic histology based on pattern classification. Journal of Pathology Informatics, 2013, 4, 3.	0.8	7

108 Efficient nonrigid registration using ranked order statistics. , 2013, , .

1

#	Article	IF	CITATIONS
109	A Transfer-Learning Approach to Image Segmentation Across Scanners by Maximizing Distribution Similarity. Lecture Notes in Computer Science, 2013, , 49-56.	1.0	8
110	Carotid Artery Wall Segmentation by Coupled Surface Graph Cuts. Lecture Notes in Computer Science, 2013, , 38-47.	1.0	6
111	Geometric Tree Kernels: Classification of COPD from Airway Tree Geometry. Lecture Notes in Computer Science, 2013, 23, 171-183.	1.0	8
112	Tree-Space Statistics and Approximations for Large-Scale Analysis of Anatomical Trees. Lecture Notes in Computer Science, 2013, 23, 74-85.	1.0	23
113	Quantitative Airway Analysis in Longitudinal Studies Using Groupwise Registration and 4D Optimal Surfaces. Lecture Notes in Computer Science, 2013, 16, 287-294.	1.0	3
114	Carotid Artery Lumen Segmentation in 3D Free-Hand Ultrasound Images Using Surface Graph Cuts. Lecture Notes in Computer Science, 2013, 16, 542-549.	1.0	7
115	Automated Brain-Tissue Segmentation by Multi-Feature SVM Classification. , 2013, , .		13
116	Distribution, Size, and Shape of Abdominal Aortic Calcified Deposits and Their Relationship to Mortality in Postmenopausal Women. International Journal of Biomedical Imaging, 2012, 2012, 1-8.	3.0	8
117	Multi-feature-based plaque characterization in <i>ex vivo</i> MRI trained by registration to 3D histology. Physics in Medicine and Biology, 2012, 57, 241-256.	1.6	11
118	Towards exaggerated emphysema stereotypes. , 2012, , .		2
119	Three-Section Expiratory CT: Insufficient for Trapped Air Assessment in Patients with Cystic Fibrosis?. Radiology, 2012, 262, 969-976.	3.6	13
120	Chest Computed Tomography Scores Are Predictive of Survival in Patients with Cystic Fibrosis Awaiting Lung Transplantation. American Journal of Respiratory and Critical Care Medicine, 2012, 185, 1096-1103.	2.5	55
121	Quantitative imaging biomarkers in neurologic disease: Population study perspective. , 2012, , .		1
122	A Genome-Wide Association Study Identifies Five Loci Influencing Facial Morphology in Europeans. PLoS Genetics, 2012, 8, e1002932.	1.5	274
123	Supervised Image Segmentation across Scanner Protocols: A Transfer Learning Approach. Lecture Notes in Computer Science, 2012, , 160-167.	1.0	7
124	Factors influencing the decline in lung density in a Danish lung cancer screening cohort. European Respiratory Journal, 2012, 40, 1142-1148.	3.1	22
125	Toward automatic regional analysis of pulmonary function using inspiration and expiration thoracic CT. Medical Physics, 2012, 39, 1650-1662.	1.6	43
126	Regression-Based Cardiac Motion Prediction From Single-Phase CTA. IEEE Transactions on Medical Imaging, 2012, 31, 1311-1325.	5.4	21

#	Article	IF	CITATIONS
127	Statistical Shape Model-Based Femur Kinematics From Biplane Fluoroscopy. IEEE Transactions on Medical Imaging, 2012, 31, 1573-1583.	5.4	21
128	Shape-based Assessment of Vertebral Fracture Risk in Postmenopausal Women Using Discriminative Shape Alignment. Academic Radiology, 2012, 19, 446-454.	1.3	2
129	A computer aided detection system for cerebral microbleeds in brain MRI. , 2012, , .		17
130	Automated measurement of local white matter lesion volume. NeuroImage, 2012, 59, 3901-3908.	2.1	14
131	Extraction of Airways From CT (EXACT'09). IEEE Transactions on Medical Imaging, 2012, 31, 2093-2107.	5.4	173
132	Supervised in-vivo plaque characterization incorporating class label uncertainty. , 2012, , .		5
133	Mass preserving image registration for lung CT. Medical Image Analysis, 2012, 16, 786-795.	7.0	67
134	Texture-Based Analysis of COPD: A Data-Driven Approach. IEEE Transactions on Medical Imaging, 2012, 31, 70-78.	5.4	78
135	Automated Brain Structure Segmentation Based on Atlas Registration and Appearance Models. IEEE Transactions on Medical Imaging, 2012, 31, 276-286.	5.4	54
136	A Hierarchical Scheme for Geodesic Anatomical Labeling of Airway Trees. Lecture Notes in Computer Science, 2012, 15, 147-155.	1.0	16
137	Plaque characterization in ex vivo MRI evaluated by dense 3D correspondence with histology. , 2011, , .		3
138	2D–3D shape reconstruction of the distal femur from stereo X-ray imaging using statistical shape models. Medical Image Analysis, 2011, 15, 840-850.	7.0	139
139	Maximum a Posteriori Estimation of Linear Shape Variation With Application to Vertebra and Cartilage Modeling. IEEE Transactions on Medical Imaging, 2011, 30, 1514-1526.	5.4	5
140	Evaluation of Registration Methods on Thoracic CT: The EMPIRE10 Challenge. IEEE Transactions on Medical Imaging, 2011, 30, 1901-1920.	5.4	363
141	Robust Shape Regression for Supervised Vessel Segmentation and its Application to Coronary Segmentation in CTA. IEEE Transactions on Medical Imaging, 2011, 30, 1974-1986.	5.4	51
142	Vertebral fracture risk (VFR) score for fracture prediction in postmenopausal women. Osteoporosis International, 2011, 22, 2119-2128.	1.3	9
143	Short-term effect of changes in smoking behaviour on emphysema quantification by CT. Thorax, 2011, 66, 55-60.	2.7	70
144	Geometries on Spaces of Treelike Shapes. Lecture Notes in Computer Science, 2011, , 160-173.	1.0	15

#	Article	IF	CITATIONS
145	Optimal Graph Based Segmentation Using Flow Lines with Application to Airway Wall Segmentation. Lecture Notes in Computer Science, 2011, 22, 49-60.	1.0	23
146	Improved Tissue Segmentation by Including an MR Acquisition Model. Lecture Notes in Computer Science, 2011, , 152-159.	1.0	1
147	Multiple Classifier Systems in Texton-Based Approach for the Classification of CT Images of Lung. Lecture Notes in Computer Science, 2011, , 153-163.	1.0	5
148	Comparison of Shape Regression Methods under Landmark Position Uncertainty. Lecture Notes in Computer Science, 2011, 14, 434-441.	1.0	7
149	Dissimilarity-Based Classification of Anatomical Tree Structures. Lecture Notes in Computer Science, 2011, 22, 475-485.	1.0	5
150	Quantitative analysis of airway abnormalities in CT. , 2010, , .		7
151	MACD: an imaging marker for cardiovascular disease. Proceedings of SPIE, 2010, , .	0.8	Ο
152	Quantitative Analysis of Pulmonary Emphysema Using Local Binary Patterns. IEEE Transactions on Medical Imaging, 2010, 29, 559-569.	5.4	319
153	Distribution, size, shape, growth potential and extent of abdominal aortic calcified deposits predict mortality in postmenopausal women. BMC Cardiovascular Disorders, 2010, 10, 56.	0.7	11
154	Vessel-guided airway tree segmentation: A voxel classification approach. Medical Image Analysis, 2010, 14, 527-538.	7.0	112
155	Confidence of model based shape reconstruction from sparse data. , 2010, , .		8
156	Lung CT registration combining intensity, curves and surfaces. , 2010, , .		9
157	Early diagnosis of dementia based on intersubject whole-brain dissimilarities. , 2010, , .		12
158	Vessel tree extraction using locally optimal paths. , 2010, , .		16
159	Dissimilarity-Based Multiple Instance Learning. Lecture Notes in Computer Science, 2010, , 129-138.	1.0	8
160	Image Dissimilarity-Based Quantification of Lung Disease from CT. Lecture Notes in Computer Science, 2010, 13, 37-44.	1.0	15
161	Conditional Shape Models for Cardiac Motion Estimation. Lecture Notes in Computer Science, 2010, 13, 452-459.	1.0	9
162	A Texton-Based Approach for the Classification of Lung Parenchyma in CT Images. Lecture Notes in Computer Science, 2010, 13, 595-602.	1.0	63

#	Article	IF	CITATIONS
163	Prediction of Dementia by Hippocampal Shape Analysis. Lecture Notes in Computer Science, 2010, , 42-49.	1.0	4
164	Early Detection of Emphysema Progression. Lecture Notes in Computer Science, 2010, 13, 193-200.	1.0	6
165	Mass preserving registration for lung CT. , 2009, , .		2
166	Cystic Fibrosis: Are Volumetric Ultra-Low-Dose Expiratory CT Scans Sufficient for Monitoring Related Lung Disease?. Radiology, 2009, 253, 223-229.	3.6	82
167	Bicycle chain shape models. , 2009, , .		7
168	Cerebellum segmentation in MRI using atlas registration and local multi-scale image descriptors. , 2009, , .		15
169	Dissimilarity representations in lung parenchyma classification. , 2009, , .		5
170	Discriminative Shape Alignment. Lecture Notes in Computer Science, 2009, 21, 459-466.	1.0	4
171	Airway Tree Extraction with Locally Optimal Paths. Lecture Notes in Computer Science, 2009, 12, 51-58.	1.0	18
172	Learning COPD Sensitive Filters in Pulmonary CT. Lecture Notes in Computer Science, 2009, 12, 699-706.	1.0	8
173	Bicycle chain shape models. , 2009, , .		2
174	Special Issue on Tribute Workshop for Peter Johansen. Journal of Mathematical Imaging and Vision, 2008, 31, 119-120.	0.8	0
175	Multi-object tracking of human spermatozoa. , 2008, , .		14
176	Supervised shape analysis for risk assessment in osteoporosis. , 2008, , .		2
177	Voxel classification based airway tree segmentation. Proceedings of SPIE, 2008, , .	0.8	10
178	Integrating local voxel classification and global shape models for medical image segmentation. Proceedings of SPIE, 2008, , .	0.8	0
179	Texture Classification in Lung CT Using Local Binary Patterns. Lecture Notes in Computer Science, 2008, 11, 934-941.	1.0	28
180	Weight Preserving Image Registration for Monitoring Disease Progression in Lung CT. Lecture Notes in Computer Science, 2008, 11, 863-870.	1.0	37

#	Article	IF	CITATIONS
181	Vertebral fracture classification. , 2007, , .		3
182	Semiautomatic Segmentation of Vertebrae in Lateral X-rays Using a Conditional Shape Model. Academic Radiology, 2007, 14, 1156-1165.	1.3	21
183	Quantitative vertebral morphometry using neighbor-conditional shape models. Medical Image Analysis, 2007, 11, 503-512.	7.0	55
184	A computer-based measure of irregularity in vertebral alignment is a BMD-independent predictor of fracture risk in postmenopausal women. Osteoporosis International, 2007, 18, 1525-1530.	1.3	7
185	Quantifying Calcification in the Lumbar Aorta on X-Ray Images. Lecture Notes in Computer Science, 2007, 10, 352-359.	1.0	3
186	Toward automated detection and segmentation of aortic calcifications from radiographs. , 2007, , .		3
187	A Family of Principal Component Analyses for Dealing with Outliers. Lecture Notes in Computer Science, 2007, 10, 178-185.	1.0	5
188	A pixelwise inpainting-based refinement scheme for quantizing calcification in the lumbar aorta on 2D lateral x-ray images. , 2006, 6144, 474.		1
189	Quantitative Vertebral Morphometry Using Neighbor-Conditional Shape Models. Lecture Notes in Computer Science, 2006, 9, 1-8.	1.0	12
190	Shape regression for vertebra fracture quantification. , 2005, , .		3
191	Multi-object Segmentation Using Shape Particles. Lecture Notes in Computer Science, 2005, 19, 762-773.	1.0	8
192	A Pattern Classification Approach to Aorta Calcium Scoring in Radiographs. Lecture Notes in Computer Science, 2005, , 170-177.	1.0	4
193	Quantizing Calcification in the Lumbar Aorta on 2-D Lateral X-Ray Images. Lecture Notes in Computer Science, 2005, , 409-418.	1.0	5
194	Image segmentation by shape particle filtering. , 2004, , .		29
195	Interactive segmentation of abdominal aortic aneurysms in CTA images. Medical Image Analysis, 2004, 8, 127-138.	7.0	105
196	Shape Particle Filtering for Image Segmentation. Lecture Notes in Computer Science, 2004, , 168-175.	1.0	27
197	Localization and segmentation of aortic endografts using marker detection. IEEE Transactions on Medical Imaging, 2003, 22, 473-482.	5.4	6
198	Adapting Active Shape Models for 3D Segmentation of Tubular Structures in Medical Images. Lecture Notes in Computer Science, 2003, 18, 136-147.	1.0	97

#	Article	IF	CITATIONS
199	Interactive shape models. , 2003, 5032, 1206.		10
200	Model-based segmentation of abdominal aortic aneurysms in CTA images. , 2003, , .		10
201	Automated Segmentation of Abdominal Aortic Aneurysms in Multi-spectral MR Images. Lecture Notes in Computer Science, 2003, , 538-545.	1.0	6
202	Active-shape-model-based segmentation of abdominal aortic aneurysms in CTA images. , 2002, , .		30
203	Measurements of the current density profile with tangential Thomson scattering in RTP. Plasma Physics and Controlled Fusion, 2001, 43, 443-468.	0.9	6
204	<title>Semiautomatic aortic endograft localization for postoperative evaluation of endovascular aneurysm treatment</title> . , 2001, , .		3
205	Shape Particle Guided Tissue Classification. , 0, , .		7
206	MRI changes in diaphragmatic motion and curvature in Pompe disease over time. European Radiology, 0,	2.3	0